

Electronic Supplementary Information

Hypochlorous acid triggered fluorescent probes for in situ imaging of psoriasis model

Peng Wei^{a,b}, Yu Guo^a, Lingyan Liu^a, Xiaojun Zhou^{*a} and Tao Yi^{*a,b}

^aState Key Laboratory for Modification of Chemical Fibers and Polymer Materials, Shanghai Engineering Research Center of Nano-Biomaterials and Regenerative Medicine, College of Chemistry, Chemical Engineering and Biotechnology, Donghua University, Shanghai 201620, China

^bNational Innovation Center of Advanced Dyeing and Finishing Technology, Tai'an, Shandong 271000, P.R.China

Corresponding author. E-mail address: zxj@dhu.edu.cn; yitao@dhu.edu.cn

Table of contents

1 The synthesis of the compounds.....	2
1.1 The synthesis of G1	2
2.2 The synthesis of G2	2
3 Additional figures	4
3 NMR and HRMS spectra.....	14
4 References.....	18

1 The synthesis of the compounds

The synthesis route of **G1** and **G2** were similar to our reported procedure and shown in **Scheme 1**.¹

1.1 The synthesis of **G1**

To an aqueous solution (20 mL) of Oxazine 1 (1.59 g, 3.75 mmol, 1.0 eq), dichloromethane (15 mL) and Na₂CO₃ (2.38 g, 22.50 mmol, 6.0 eq) were added and stirred at 40°C under a nitrogen atmosphere. Sodium dithionite (2.61 g, 15.00 mmol, 4.0 eq) was dissolved in 15 mL of water and added dropwise. After addition the mixture was stirred at 40°C under nitrogen atmosphere until the solution became yellow (typically within 15-30 min). The dichloromethane layer was separated from water layer and dried with anhydrous sodium sulfate quickly. After sodium sulfate was removed by filtration, the solution was added dropwise to a mixture of acetyl chloride (5.63 mmol, 1.5 eq), Na₂CO₃ (1.19 g, 11.25 mmol, 3.0 eq) in 5 mL dichloromethane. After addition the mixture was stirred in an ice-water bath for 0.5 h and then at room temperature until the reaction completed as indicated by TLC analysis.

Removing the undissolved substance by filtration, the solution was poured into 200 mL of ice-water while stirring, and the resulting mixture was extracted with 3 × 100 mL portions of ethyl acetate. The combined extracts were washed with brine, dried over anhydrous sodium sulfate and evaporated on a rotary evaporator to afford a solid residue, which was purified by column chromatography (ethyl acetate/n-hexane = 1/3) to yield **G1** as a white solid.

¹H NMR (400 MHz, CD₃CN) δ 7.25 (d, *J* = 9.2 Hz, 2H), 6.42 (dd, *J* = 8.8, 2.8 Hz, 2H), 6.38 (d, *J* = 2.8 Hz, 2H), 3.35 (q, *J* = 7.0 Hz, 8H), 2.17 (s, 3H), 1.12 (t, *J* = 7.0 Hz, 12H).

¹³C NMR (100 MHz, CDCl₃) δ 169.7, 152.1, 146.8, 125.4, 118.4, 106.3, 99.7, 44.7, 23.0, 12.6.

HRMS (ESI): calcd for C₂₂H₂₉N₃O₂ [M + H]⁺: 368.2333; found: 368.2338.

2.2 The synthesis of **G2**

To an aqueous solution (20 mL) of Oxazine 1 (1.59 g, 3.75 mmol, 1.0 eq), dichloromethane (15 mL) and Na₂CO₃ (2.38 g, 22.50 mmol, 6.0 eq) were added and stirred at 40°C under a nitrogen atmosphere. Sodium dithionite (2.61 g, 15.00 mmol, 4.0 eq) was dissolved in 15 mL of water and added dropwise. After addition the mixture was stirred at 40°C under nitrogen atmosphere until the solution became

yellow. The mixture was cooled with an ice-water bath, to which a dichloromethane solution (5 mL) of bis(trichloromethyl)carbonate (1.11 g, 3.75 mmol, 1.0 eq) was added dropwise. After addition, the mixture was stirred for another 1 h. The dichloromethane layer was separated from the water layer and quickly dried with anhydrous sodium sulfate. After sodium sulfate was removed by filtration, the solution was added dropwise to a mixture of 4-(2-aminoethyl) morpholine (3 mL) and 5 mL dichloromethane. After addition, the mixture was stirred in an ice-water bath for 1 h and then at room temperature until the reaction was completed as indicated by TLC analysis.

The solution was poured into 200 mL of ice-water while stirring, and the resulting mixture was extracted with three 100 mL portions of ethyl acetate. The combined extracts were washed with brine, dried over anhydrous sodium sulfate and evaporated on a rotary evaporator to afford an residue, which was purified by column chromatography (ethyl acetate/n-hexane = 1/10 then 1/5) to yield **G2** as white solids.

^1H NMR (400 MHz, CD_3CN) δ 7.22 (d, J = 8.8 Hz, 2H), 6.44 (d, J = 8.8 Hz, 2H), 6.37 (s, 2H), 6.07 (s, 1H), 3.53 (s, 4H), 3.35 (q, J = 7.0 Hz, 8H), 3.21 (dd, J = 10.8, 5.6 Hz, 2H), 2.40 (t, J = 6.2 Hz, 2H), 2.35 (s, 4H), 1.13 (t, J = 7.0 Hz, 12H).

^{13}C NMR (100 MHz, $\text{DMSO-}d_6$) δ 155.2, 151.5, 145.9, 125.2, 117.7, 106.5, 99.2, 66.3, 56.6, 52.9, 43.8, 36.8, 12.3.

HRMS (ESI): calcd for $\text{C}_{27}\text{H}_{39}\text{N}_5\text{O}_3$ $[\text{M} + \text{H}]^+$: 482.3126; found: 482.3134.

3 Additional figures

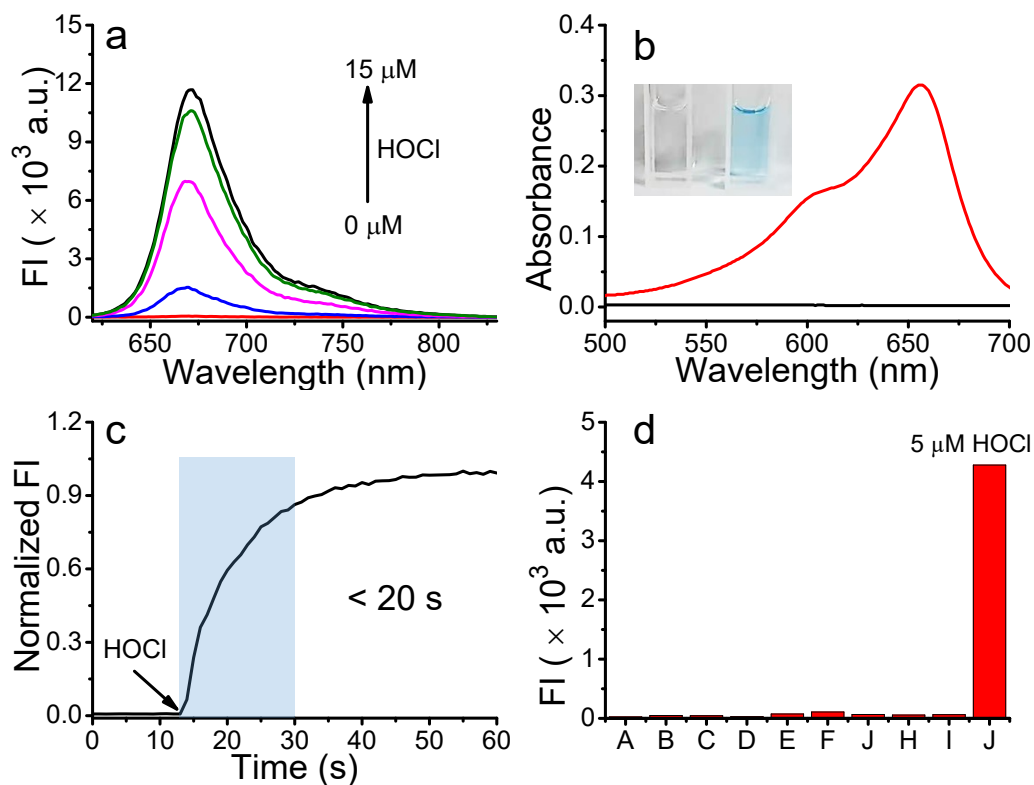


Fig. S1. (a) Fluorescence spectra of **G1** (5 μM) before/after addition of different concentration of HOCl (0, 1, 5, 10 and 15 μM). (b) Absorption spectra of **G1** (5 μM) before/after addition of 15 μM HOCl (Inset in b is the color image before (left) and after (right) treated with HOCl). (c) Time-dependent fluorescence intensity changes of **G1** (5 μM) at 669 nm upon addition of 15 μM HOCl (time range 0–60 s; $\lambda_{\text{ex}} = 610$ nm). (d) Fluorescent intensity of **G1** (5 μM) at 669 nm after treated with HOCl (5 μM) and different ROS/RNS (20 μM) (from A to I: blank, TBHP, H_2O_2 , NO, $\cdot\text{OH}$, ONOO^- , O_2^- , ROO^\cdot , t-BuOO $^\cdot$)

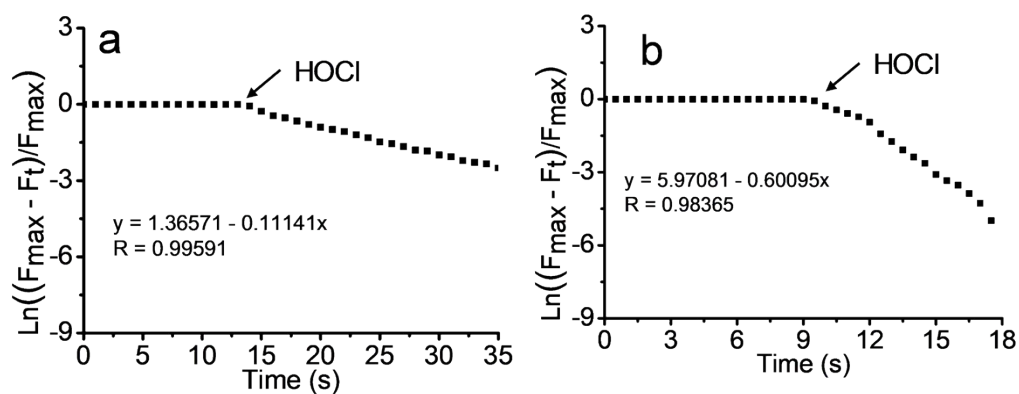


Fig. S2. Pseudo-first-order kinetic plot of the reaction of (a) 5 μM **G1** to 15 μM HOCl and (b) 5 μM **G2** to 5 μM HOCl (**G1**: slope = -0.11141, **G2**: slope = -0.60095, λ_{ex} = 610 nm).

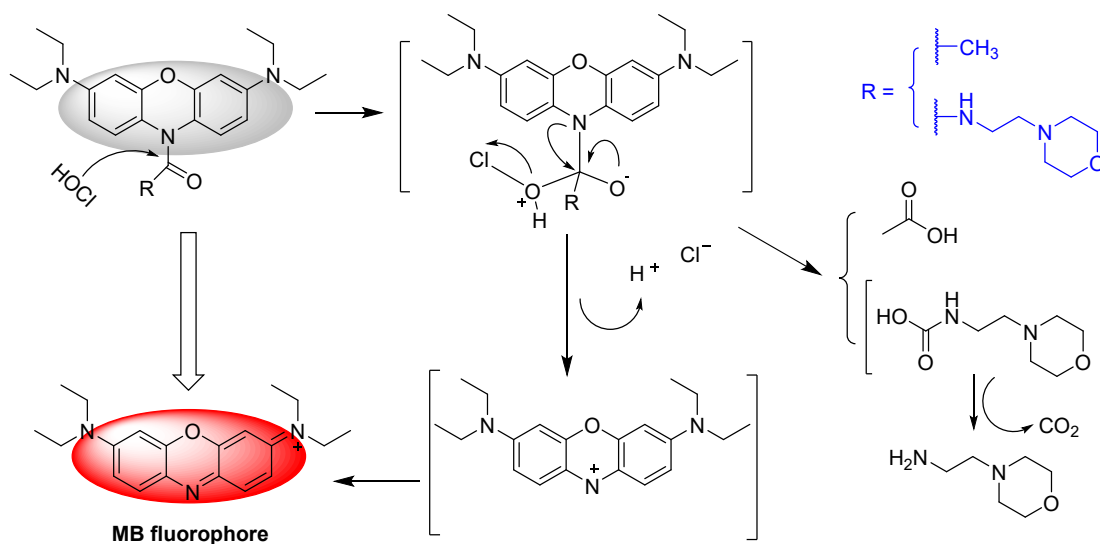


Fig. S3. The proposed mechanism of **G1** and **G2** toward HOCl

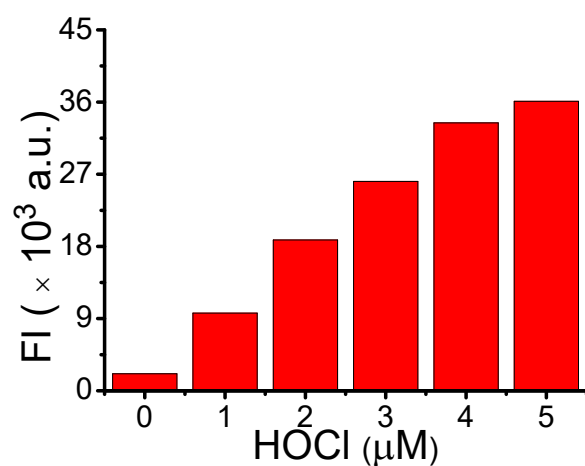


Fig. S4. Fluorescence intensity of **G2** (5 μM) at 669 nm after adding various concentrations of HOCl (0, 1, 2, 3, 4 and 5 μM)

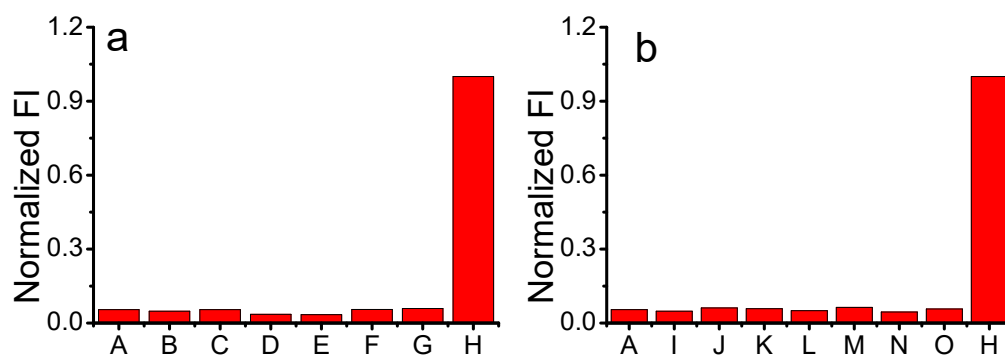


Fig. S5. (a) Fluorescent intensity of **G1** (5 μM) at 669 nm after treated with HOCl (5 μM) or different (a) anions (50 μM), (b) cations (50 μM) (A and H are Blank and HOCl (5 μM), respectively; from B to G: Cl⁻, F⁻, CH₃COO⁻, CO₃²⁻, SO₄²⁻, ClO₄⁻; from I to O: Na⁺, K⁺, Ca²⁺, Fe³⁺, Ni²⁺, Mg²⁺, Al³⁺)

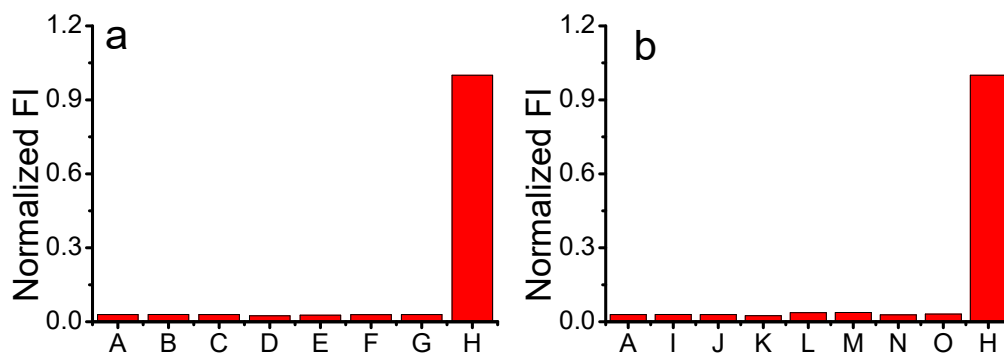


Fig. S6. (a) Fluorescent intensity of **G2** (5 μM) at 669 nm after treated with HOCl (5 μM) or different (a) anions (50 μM), (b) cations (50 μM) (A and H are Blank and HOCl (5 μM), respectively; from B to G: Cl⁻, F⁻, CH₃COO⁻, CO₃²⁻, SO₄²⁻, ClO₄⁻; from I to O: Na⁺, K⁺, Ca²⁺, Fe³⁺, Ni²⁺, Mg²⁺, Al³⁺)

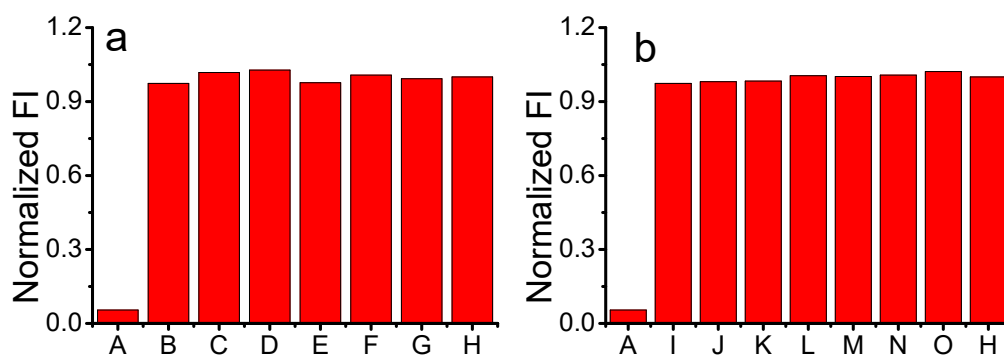


Fig. S7. (a) Fluorescent intensity of **G1** (5 μM) at 669 nm after treated with HOCl (5 μM) and different (a) anions or (b) cations (50 μM) (A: **G1** only, H: 5 μM **G1** + 5 μM HOCl. From B to G: Cl⁻, F⁻, CH₃COO⁻, CO₃²⁻, SO₄²⁻, ClO₄⁻. From I to O: Na⁺, K⁺, Ca²⁺, Fe³⁺, Ni²⁺, Mg²⁺, Al³⁺)

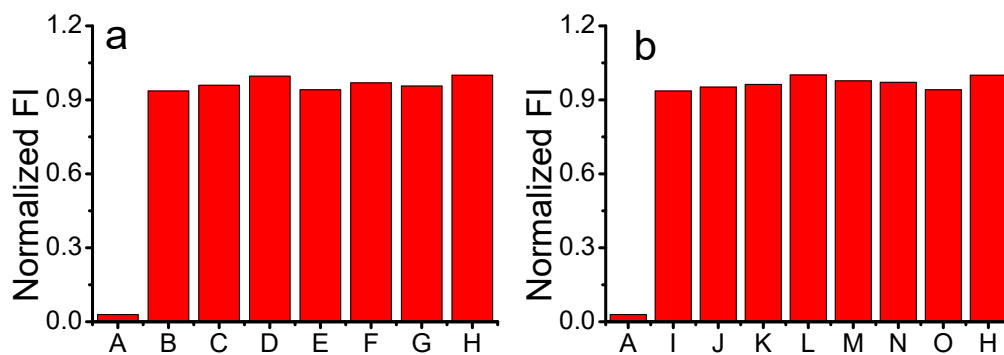


Fig. S8. Fluorescent intensity of **G2** (5 μM) at 669 nm after treated with HOCl (5 μM) and different (a) anions or (b) cations (50 μM) (A: **G2** only, H: 5 μM **G2** + 5 μM HOCl. From B to G: Cl⁻, F⁻, CH₃COO⁻, CO₃²⁻, SO₄²⁻, ClO₄⁻. From I to O: Na⁺, K⁺, Ca²⁺, Fe³⁺, Ni²⁺, Mg²⁺, Al³⁺)

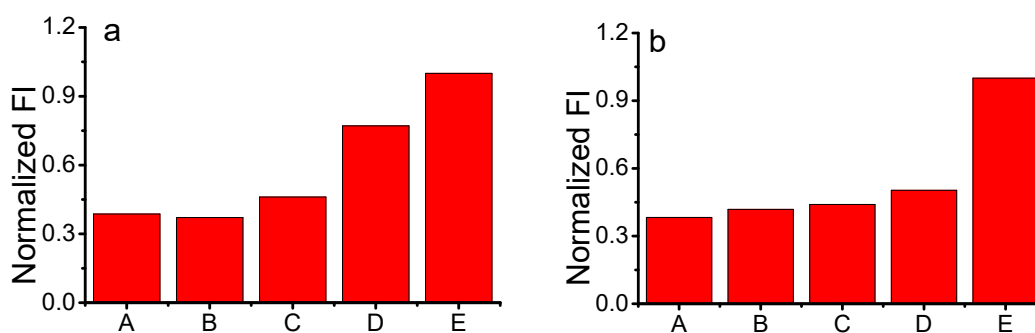


Fig. S9. Fluorescent intensity of **G1** (5 μM) at 669 nm after treated with (a) CYS (15 μM) and different concentrations of HOCl (From A to E: 5 μM **G1** only, 5 μM **G1** + 15 μM CYS, 5 μM **G1** + 15 μM CYS + 10 μM HOCl, 5 μM **G1** + 15 μM CYS + 20 μM HOCl, 5 μM **G1** + 15 μM CYS + 30 μM HOCl), and (b) GSH (15 μM) and different concentrations of HOCl (From A to E: 5 μM **G1** only, 5 μM **G1** + 15 μM GSH, 5 μM **G1** + 15 μM GSH + 10 μM HOCl, 5 μM **G1** + 15 μM GSH + 20 μM HOCl, 5 μM **G1** + 15 μM GSH + 30 μM HOCl)

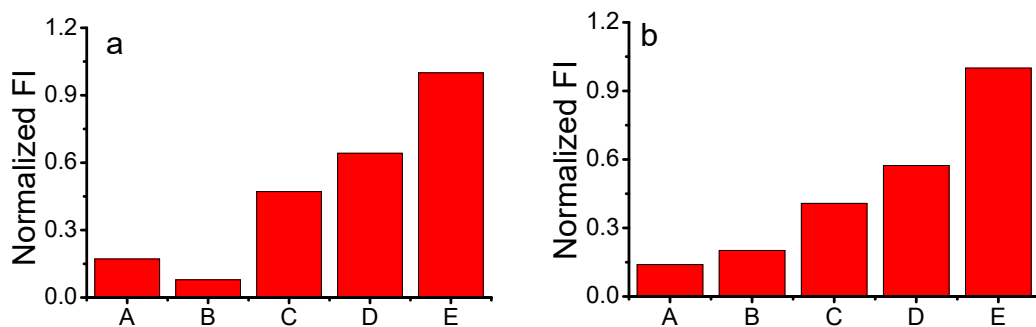


Fig. S10. Fluorescent intensity of **G2** (5 μM) at 669 nm after treated with (a) **CYS** (15 μM) and different concentrations of **HOCl** (From A to E: 5 μM **G2** only, 5 μM **G2** + 15 μM **CYS**, 5 μM **G2** + 15 μM **CYS** + 5 μM **HOCl**, 5 μM **G2** + 15 μM **CYS** + 10 μM **HOCl**, 5 μM **G2** + 15 μM **CYS** + 15 μM **HOCl**), and (b) **GSH** (15 μM) and different concentrations of **HOCl** (From A to E: 5 μM **G2** only, 5 μM **G2** + 15 μM **GSH**, 5 μM **G2** + 15 μM **GSH** + 5 μM **HOCl**, 5 μM **G2** + 15 μM **GSH** + 10 μM **HOCl**, 5 μM **G2** + 15 μM **GSH** + 15 μM **HOCl**),

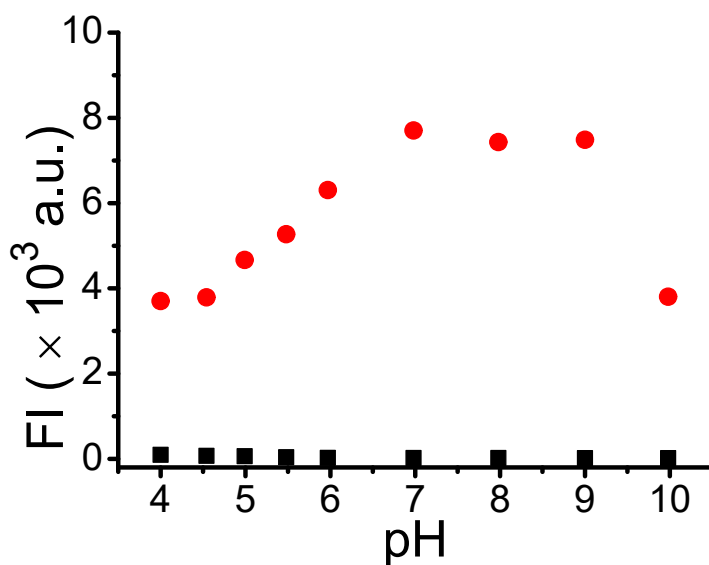


Fig. S11. Fluorescent intensity of **G1** (5 μM) at 669 nm before/after treated with **HOCl** (15 μM) at different pH.

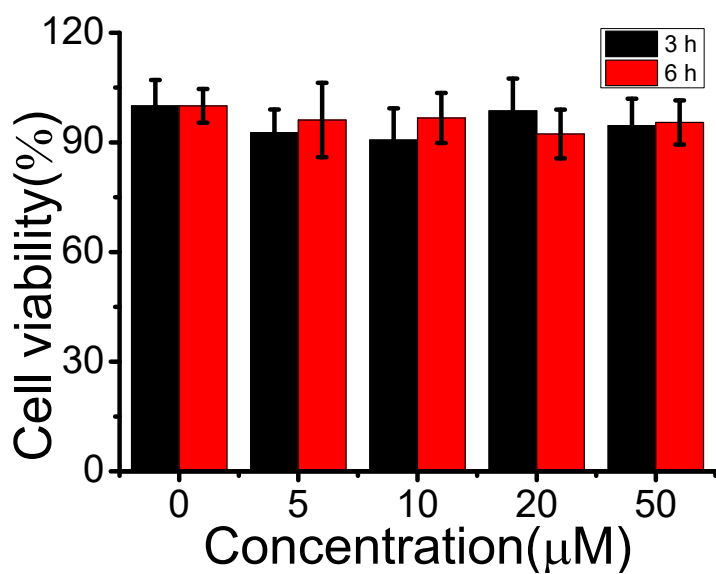


Fig. S12. The cell viability of G1 at different concentrations (0, 5, 10, 20, 50 μM) in HeLa cells for 3 h (black) and 6 h (red) measured by CCK-8 assay.

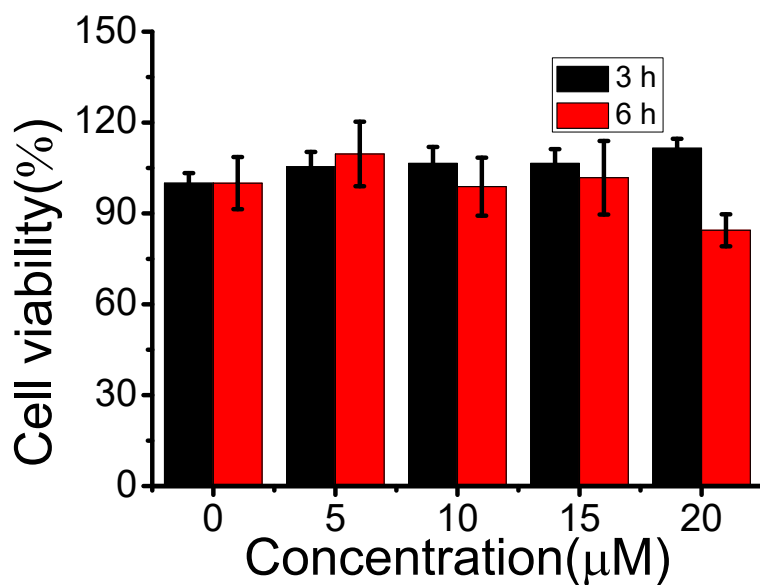


Fig. S13. The cell viability of HeLa cells after incubated with different concentrations of G2 (0, 5, 10, 15 and 20 μM) for 3 h and 6 h

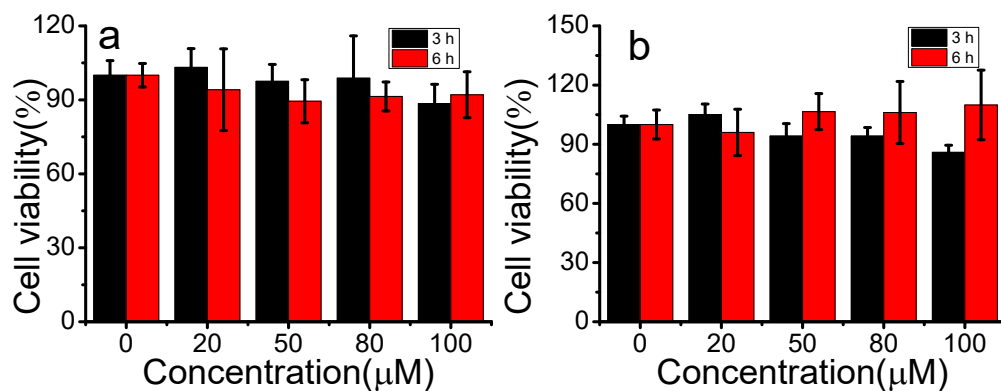


Fig. S14. The cell viability of acetic acid and 4-(2-aminoethyl)morpholine at different concentrations (0, 20, 50, 80, 100 μM) in HeLa cells for 3 h (black) and 6 h (red) measured by CCK-8 assay.

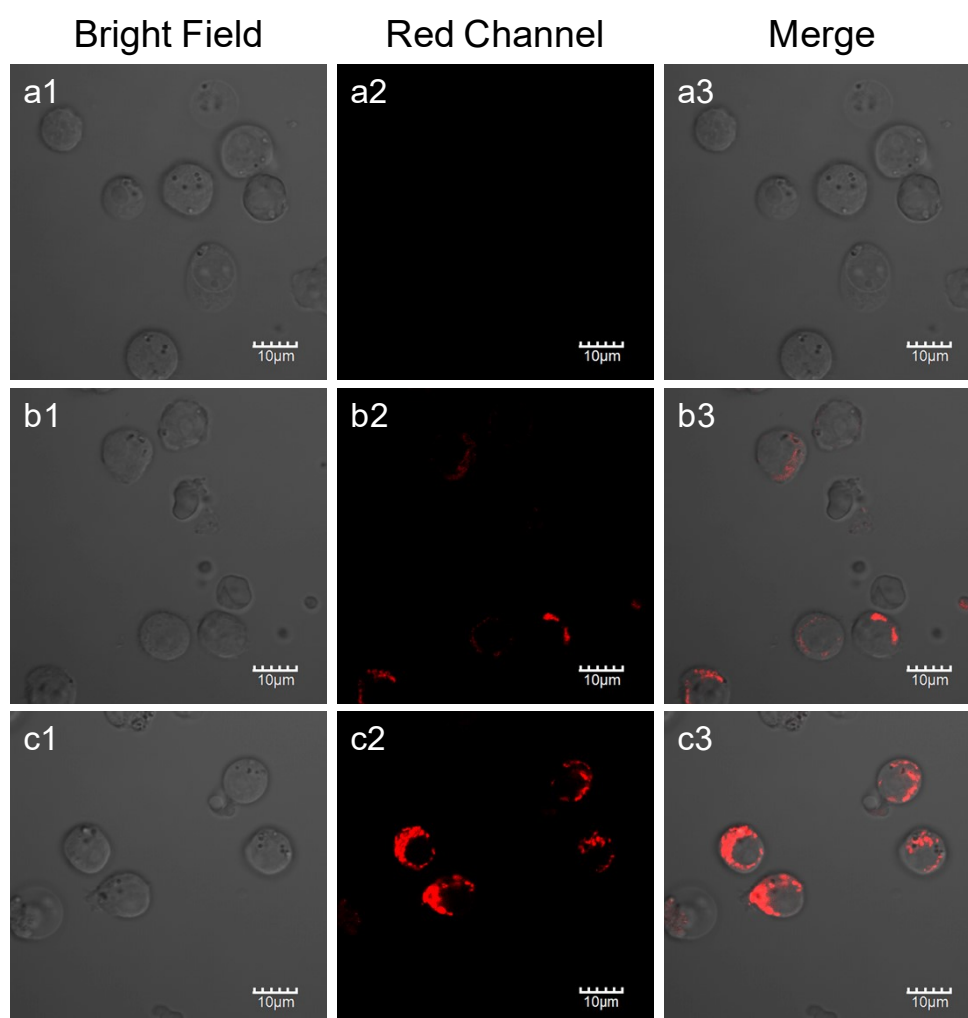


Fig. S15. CLSM images of HL-60 cells (a1, a2, a3) without any treatment; (b1, b2, b3) incubated with G2 (5 μM) for 3 h and (c1, c2, c3) 6 h. (Red channel: 700 ± 50 nm, $\lambda_{ex} = 633$ nm).

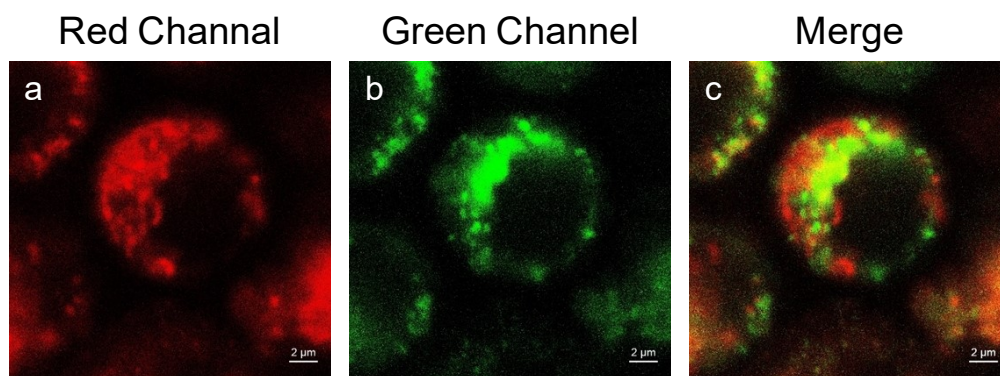


Fig. S16. CLSM images of HL-60 cells incubated with **G2** (5 μM) and DND-26 (200 nM) for 6 h (a) red channel; (b) green channel and (c) merge (Red channel: 700 ± 50 nm, $\lambda_{ex} = 633$ nm; Green channel: 530 ± 30 nm, $\lambda_{ex} = 488$ nm).

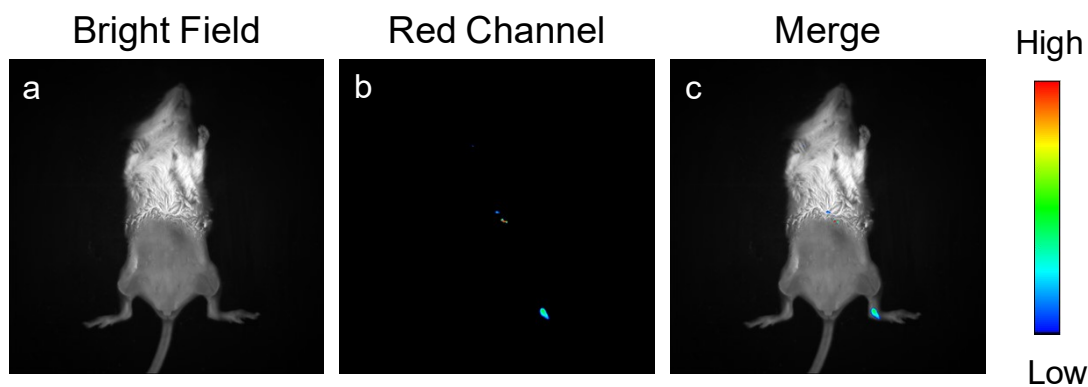


Fig. S17. *In vivo* fluorescence imaging of HOCl in a mouse model of arthritis using **G2**, (a) brightfield; (b) red channel; (c) merge. The fluorescence signal was collected at $\lambda_{em} = 650 \pm 15$ nm, 2 min after the injection of **G2**.

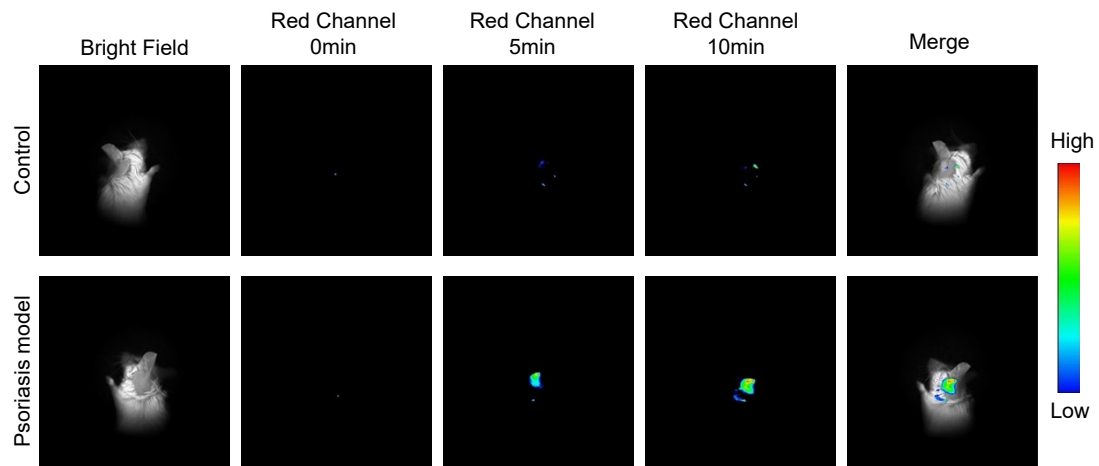
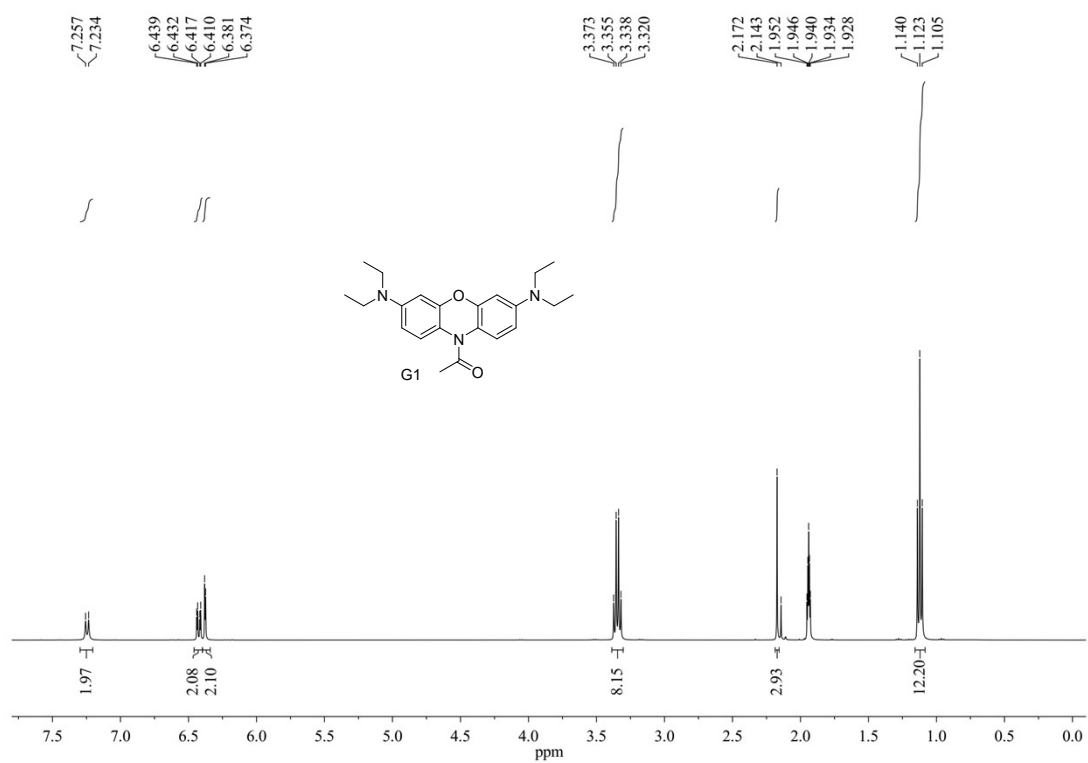
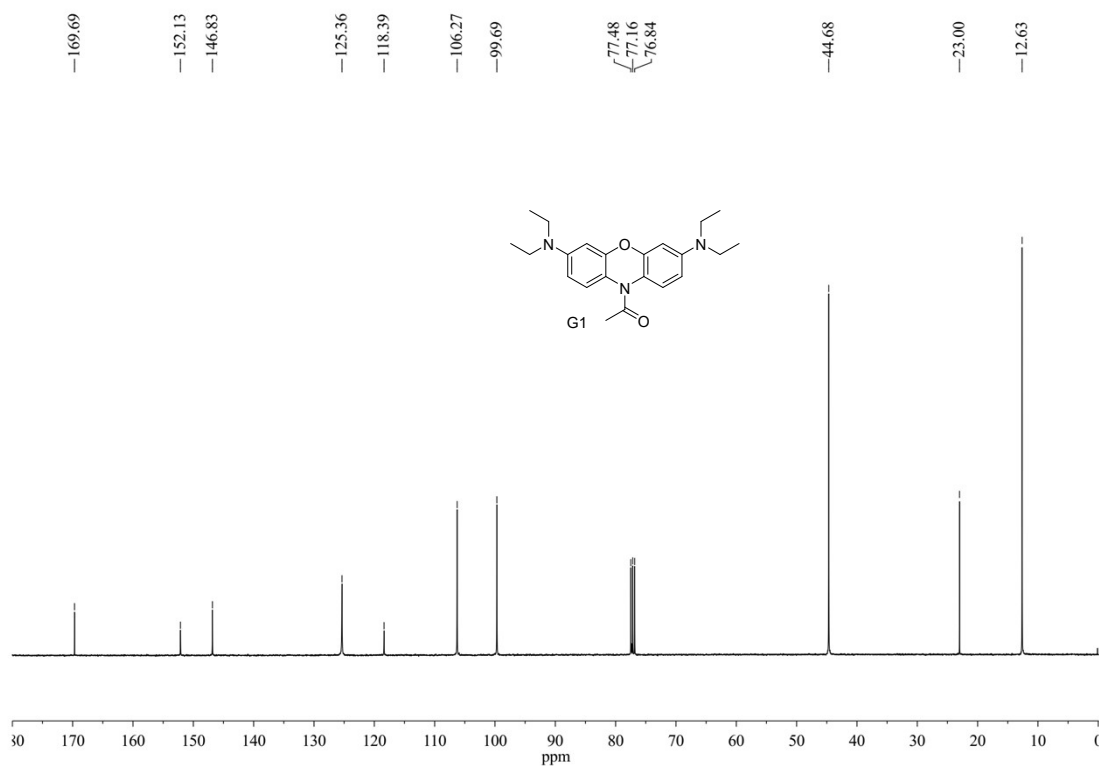


Fig. S18. *In vivo* fluorescence imaging of HOCl in a mouse model of psoriasis constructed with imiquimod using **G2**, (a1, b1, c1: brightfield; red channel and merge images of the control; a2, b2, c2: brightfield; red channel and merge images of the psoriasis model; the fluorescence signal was collected at $\lambda_{em} = 650 \pm 15$ nm, 10 min after the injection of **G2**)

3 NMR and HRMS spectra



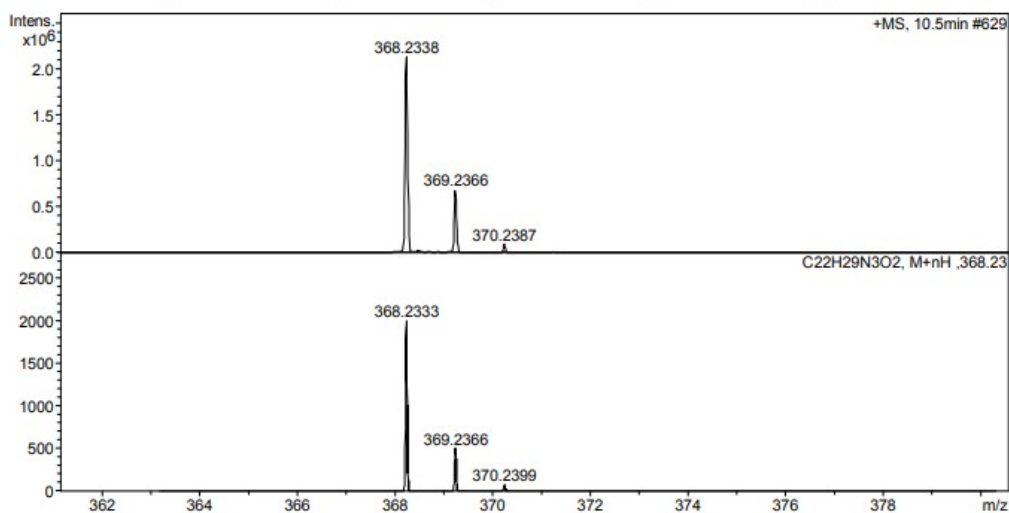
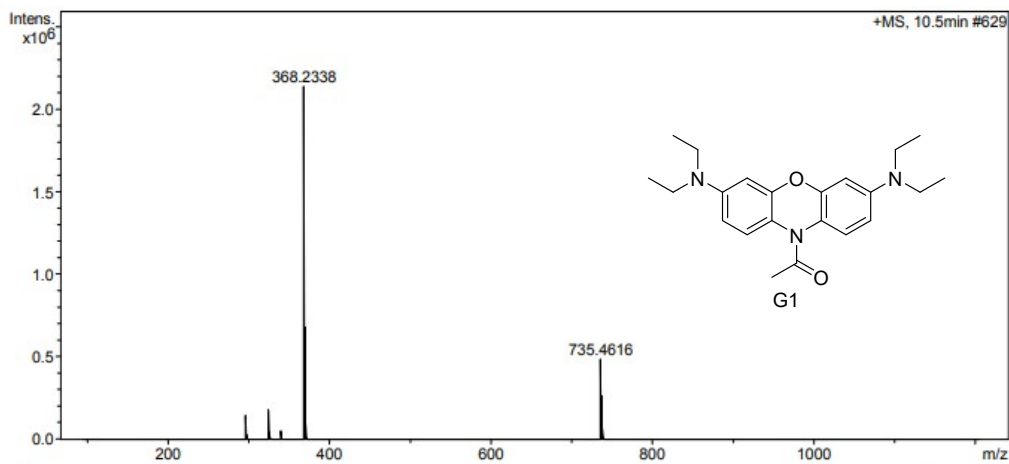
¹H NMR spectrum of **G1** in CD₃CN



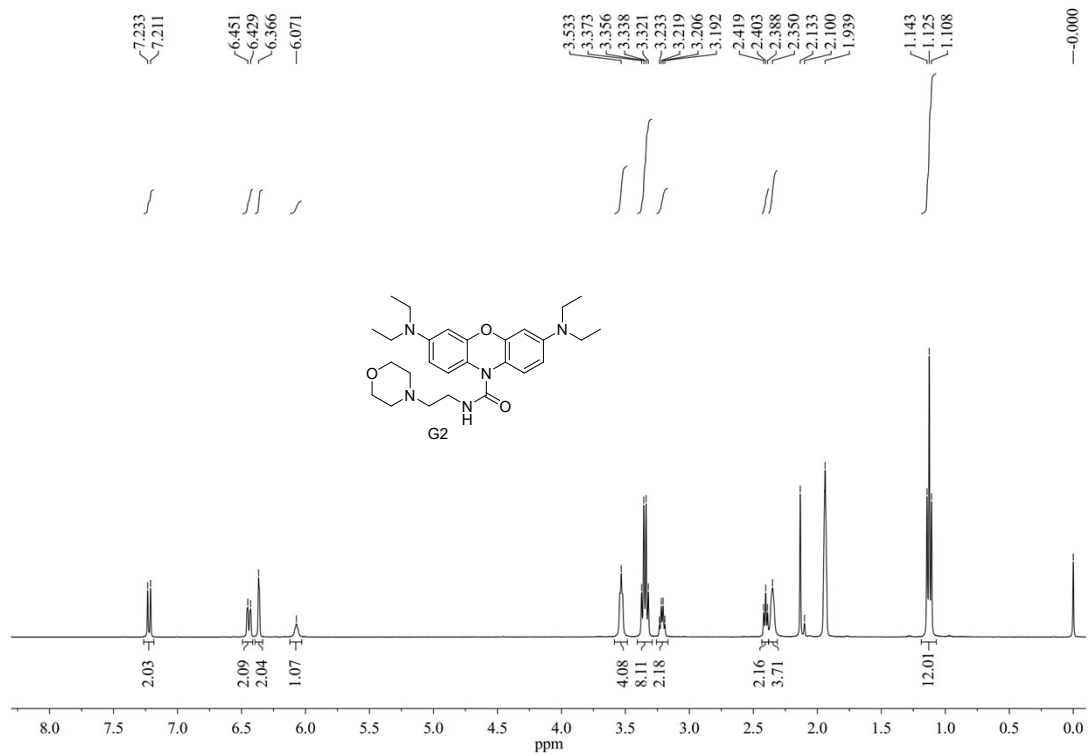
¹³C NMR spectrum of **G1** in DMSO-*d*₆

Acquisition Parameter

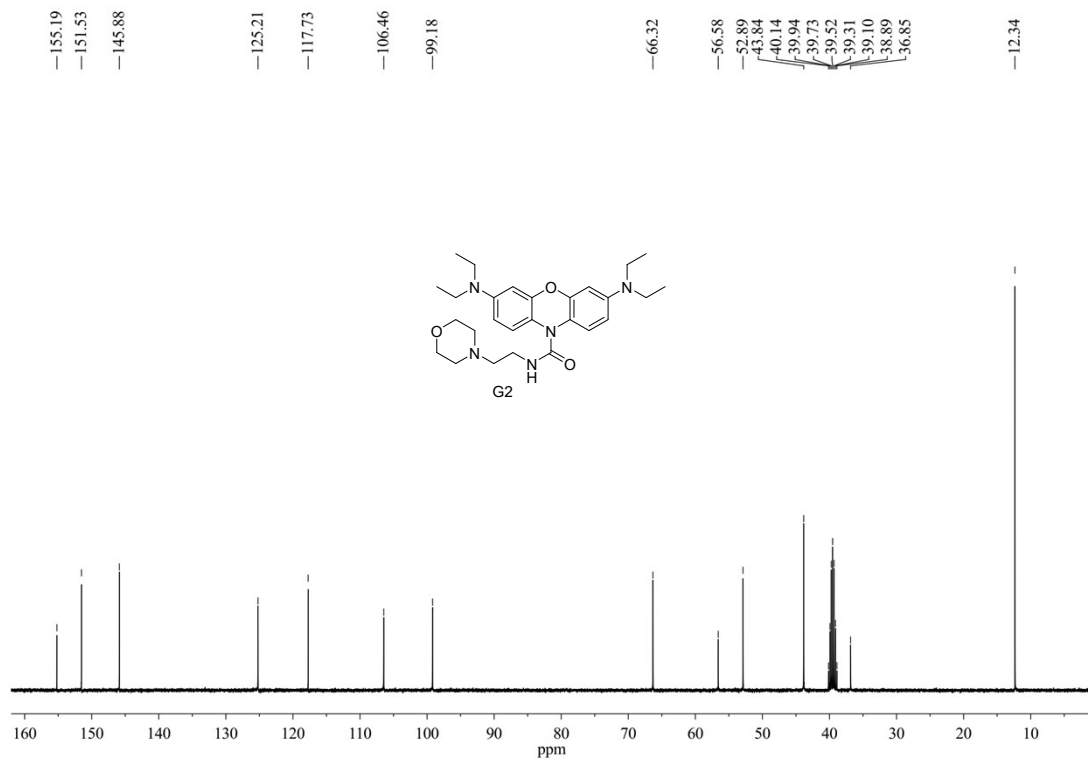
Source Type	ESI	Ion Polarity	Positive	Set Nebulizer	0.6 Bar
Focus	Not active			Set Dry Heater	200 °C
Scan Begin	100 m/z	Set Capillary	4000 V	Set Dry Gas	4.0 l/min
Scan End	1200 m/z	Set End Plate Offset	-500 V	Set Divert Valve	Waste



HRMS of G1



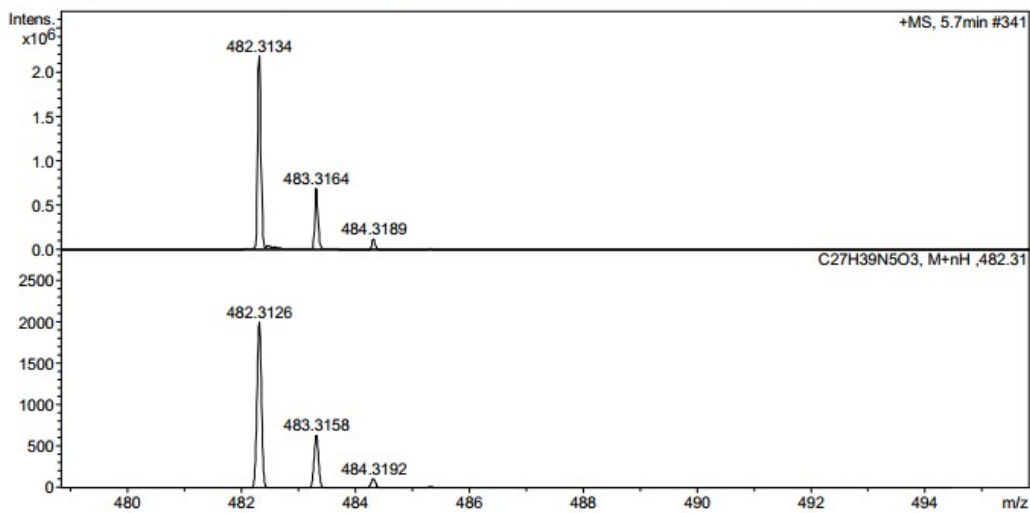
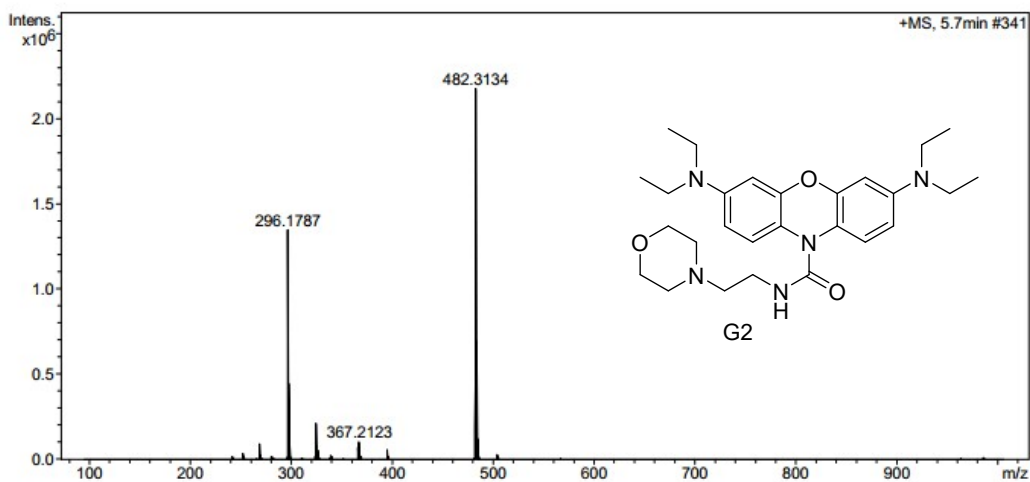
¹H NMR spectrum of G2 in CD₃CN



¹³C NMR spectrum of G2 in DMSO-*d*₆

Acquisition Parameter

Source Type	ESI	Ion Polarity	Positive	Set Nebulizer	1.0 Bar
Focus	Not active			Set Dry Heater	250 °C
Scan Begin	100 m/z	Set Capillary	4000 V	Set Dry Gas	4.0 l/min
Scan End	1000 m/z	Set End Plate Offset	-500 V	Set Divert Valve	Waste



HRMS of G2

4 References

1. P. Wei, L. Liu, Y. Wen, G. Zhao, F. Xue, W. Yuan, R. Li, Y. Zhong, M. Zhang and T. Yi, *Angew. Chem. Int. Ed.*, 2019, **58**, 4547-4551.